

SINGLE AND SUPERIMPOSED BEDFORMS: A SYNTHESIS OF SAN FRANCISCO BAY AND FLUME OBSERVATIONS

D.M. RUBIN and D.S. McCULLOCH

U.S. Geological Survey, Menlo Park, Calif. 94025 (U.S.A.)

(Received August 14, 1979)

ABSTRACT

Rubin, D.M. and McCulloch, D.S., 1980. Single and superimposed bedforms: a synthesis of San Francisco Bay and flume observations. *Sediment. Geol.*, 26: 207–231.

Tidal currents with maximum depth-averaged velocities ranging up to 250 cm/sec have generated ripples, two- and three-dimensional sand waves, and upper flat beds on the floor of central San Francisco Bay. Determination of the hydraulic conditions under which the observed beds exist, indicates that the bed configuration at any point in the bay is a function of the local velocity, sediment size, and depth. The bay observations, for flows up to 85 m deep, were combined with shallow-flow observations and a single set of bed-phase boundaries was determined for the combined data. Critical shear velocities calculated for the transitions from ripples to sand waves and from sand waves to upper flat beds, in flows tens of meters deep, are within 10% of critical shear velocities observed for the same transitions in flume flows only tens of centimeters deep.

Comparison of bedform sequences suggests that, for flows up to tens of meters deep, beds of 0.25–0.50 mm sand respond to increasing flow velocities by forming ripples, two-dimensional sand waves, three-dimensional sand waves, and flat beds. At any constant depth, equilibrium sand waves increase in height and migration rate as flow velocity increases. The wavelength and maximum height of both two- and three-dimensional sand waves increase with depth also, but migration rates decrease. Because the maximum size of both kinds of bedforms varies with depth, classification schemes based on size arbitrarily separate genetically similar bedforms.

In the bay, in contrast to flumes, sand waves having the largest height-to-depth ratios occur in relatively coarse sand. Tidal and seasonal velocity fluctuations are interpreted to be more destructive to finer-grained sand waves, because in finer grain sizes sand waves are stable at a relatively narrow range of velocities.

Ripples, sand waves, and upper and lower flat beds are commonly superimposed on larger bedforms. Small bedforms can exist in equilibrium on the larger bedforms because the large bedforms generate boundary layers in which the small bedforms are locally stable. The distribution of small bedforms superimposed on larger bedforms reflects lateral and vertical variations in shear velocity in flow over large bedforms.

INTRODUCTION

Purpose

During the past fifteen years, sedimentologists and engineers working with flumes have become better able to define the hydrodynamic conditions

under which specific bed phases are stable (Allen, 1963, 1968; Yalin, 1964; Simons et al., 1965; Guy et al., 1966; Hill, 1966; Raudkivi, 1966; Znamenskaya, 1966; Harms, 1969; Hill et al., 1969; Kennedy, 1969; Southard, 1971, 1975; Vanoni, 1974). From experiments, these workers have determined what bed phases are stable under specific combinations of depth, velocity, and sediment size, but flow depths have generally been limited to 50 cm or less. Boothroyd and Hubbard (1975) studied equilibrium bedforms and flow conditions in flows up to about 3 m deep by making direct observations in shallow estuaries in the northeast United States. Rubin and McCulloch (1976) extended bed-phase boundaries to depths of many tens of meters by observing bedforms and flow conditions in deep (up to 85 m) tidal flows in San Francisco Bay. Dalrymple et al. (1978) determined bed-phase boundaries for intermediate flow depths (3–14 m) in Bay of Fundy, Canada. The purposes of the present paper are: (1) to present observations of bedforms generated by tidal flows in central San Francisco Bay; (2) to combine those observations with shallow-flow observations to determine the relations between flow conditions, bed phase, and sand-wave height for a wide range of depths; (3) to relate bed phase to shear velocity; and (4) to relate superimposed bedforms and their distribution to vertical and lateral variations in shear velocity in flows over large bedforms.

Data sources

In flume bed-phase studies, depth, velocity, and grain size are regulated by the experimenter. Although these parameters cannot be regulated in a large-scale natural system like San Francisco Bay, they can be measured. The measurements used in the present study were compiled from four sources. Bed configuration (Fig. 1A) was mapped by side-scan sonar and precision depth recording. Grain size (Fig. 1B) was analyzed by Paul Carlson (unpubl. U.S. Geological Survey data). Depth was determined from a U.S. Coast and Geodetic Survey bathymetric chart (Fig. 1C) and from precision depth recordings. Current velocities (Fig. 1D) were measured with Roberts radio current meters by the U.S. Coast and Geodetic Survey during the 1950's.

Procedure

The bottom of the central bay was surveyed during two cruises (Fig. 2). The first, conducted when tides had the mean tidal range and tidal currents had mean maximum velocities, was a general survey of bedform distribution. During the second cruise, selected sand-wave fields were repeatedly surveyed throughout complete tide cycles when currents had velocities approaching the highest of the year.

A side-scanning-sonar system was used to obtain a three-dimensional view of the bottom for a distance of about 100 m to each side of the ship's track. Topography directly beneath the ship was recorded with a precision depth

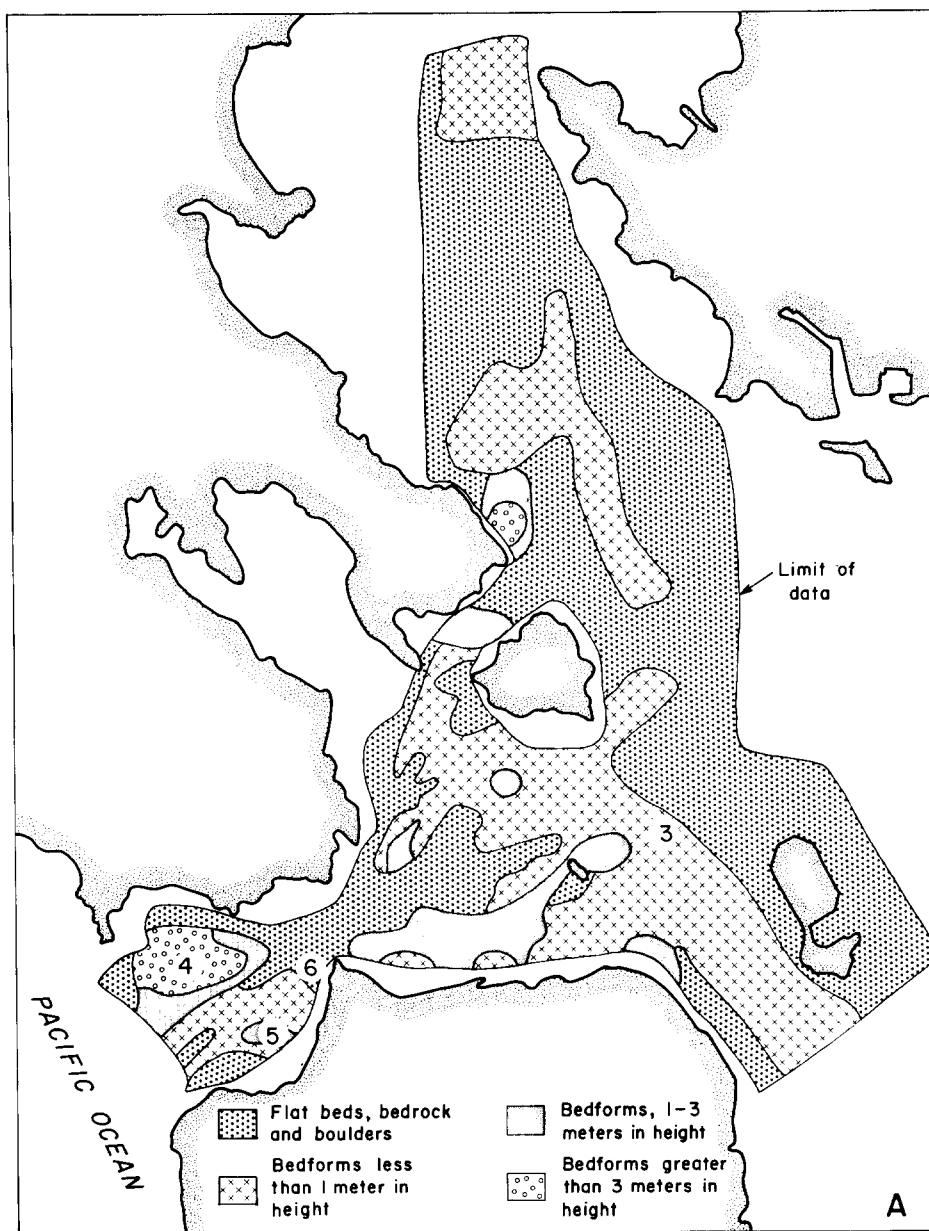


Fig. 1A. Central San Francisco Bay bed configurations. Numbers 3-6 indicate locations of bedforms shown in Figs. 3-6.

recorder, which could measure bedform height with an accuracy of about 25 cm. The ship's position was recorded continuously with an electronic dual-transponder navigation system with an accuracy of about 15 m.

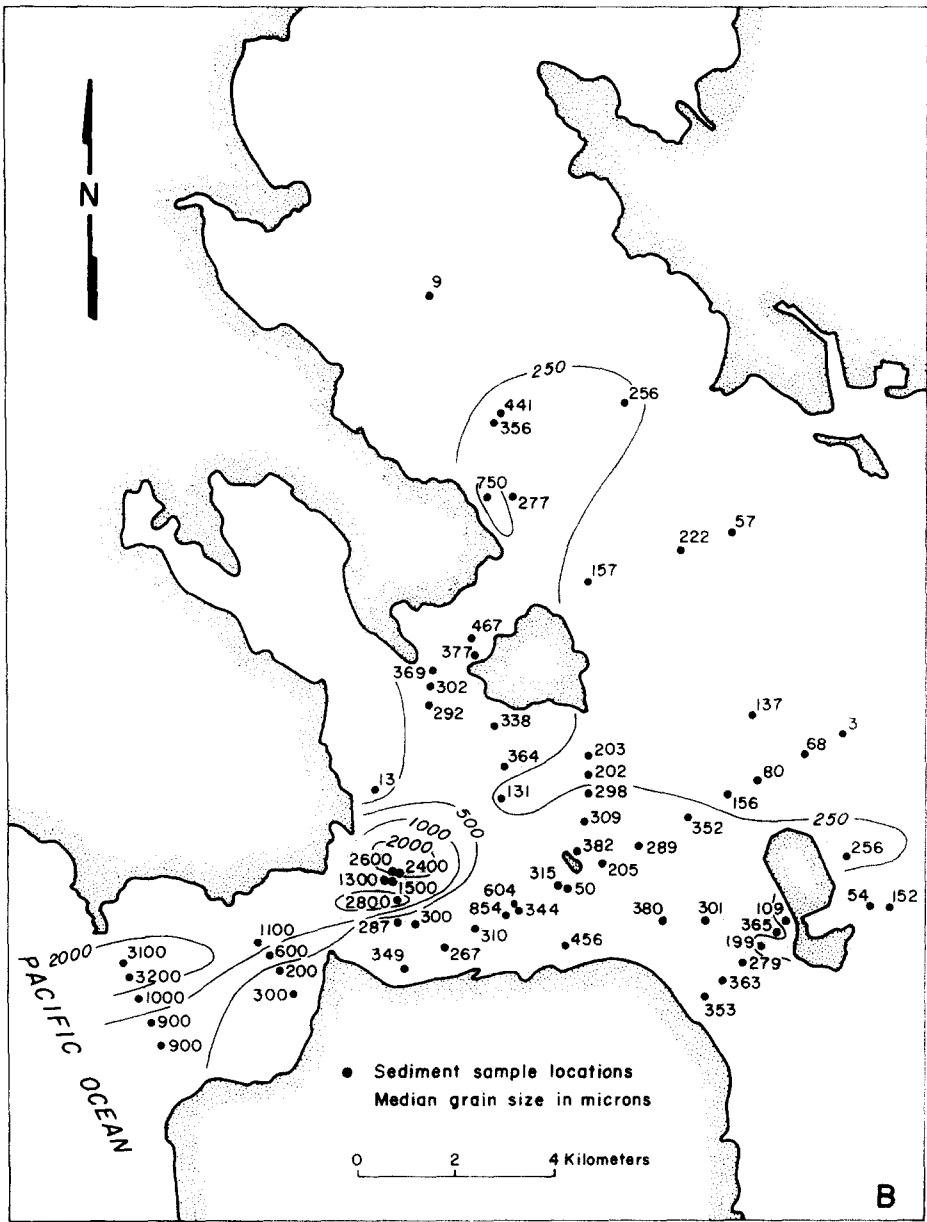


Fig. 1B. Central San Francisco Bay sediment size.

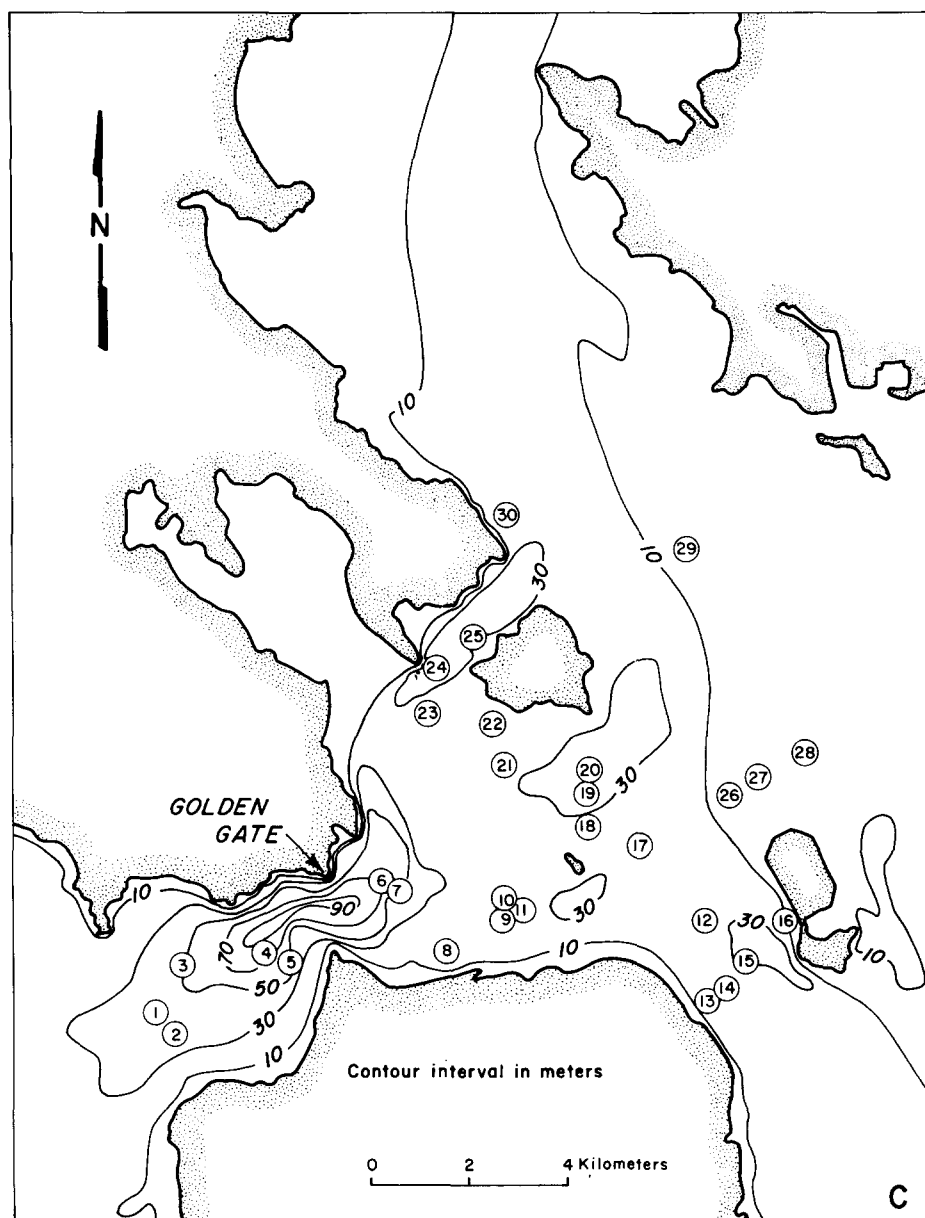


Fig. 1C. Central San Francisco Bay bathymetry. Numbers indicate locations where bed-forms and flow conditions were used in bed-phase plots (Figs. 8 and 10). Bathymetry data from U.S. Coast and Geodetic Survey.

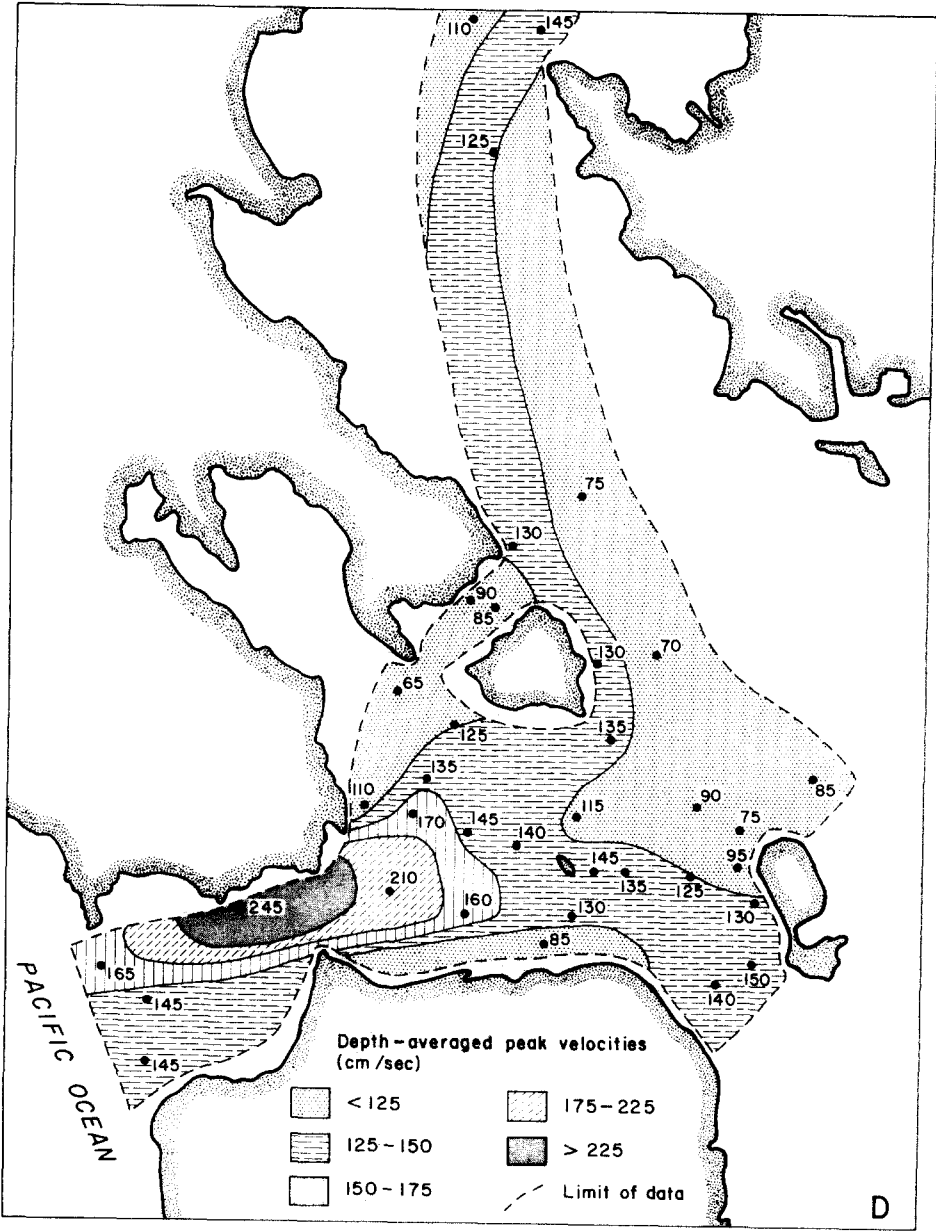


Fig. 1D. Central San Francisco Bay depth-averaged, peak-flow velocities for average tides (mean tide range $\pm 20\%$).

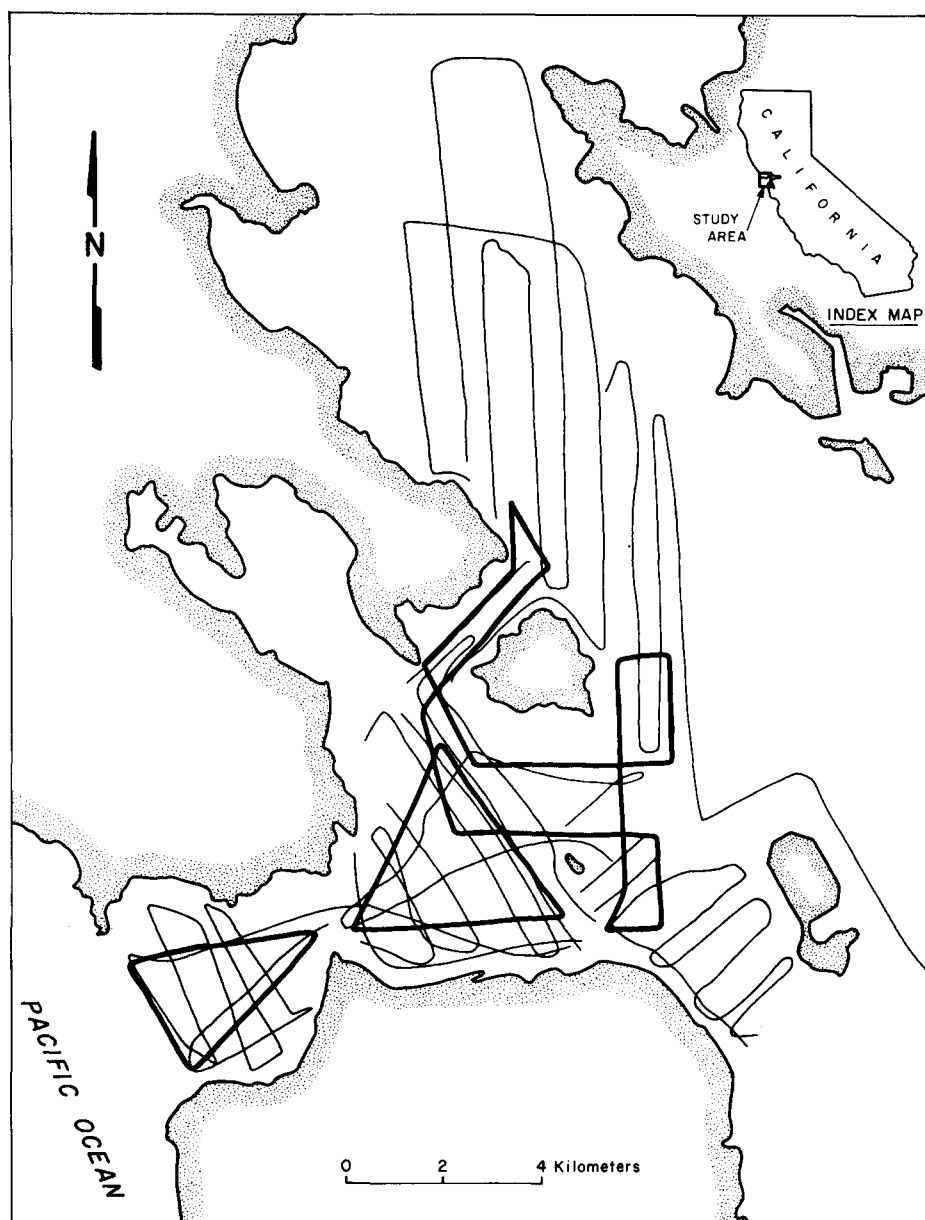


Fig. 2. Track lines. Light lines were run once, during average tides. Heavy lines were run repeatedly during spring tides.

OBSERVATIONS

Dunes and sand waves

Dunes and sand waves (transverse bedforms greater than 5 cm in height) cover approximately half of the area surveyed in the central bay (Fig. 1A). In plan view, they are straight-crested (Figs. 3 and 4), sinuous, catenary, or lunate (Fig. 5). In cross-section, they are triangular (Fig. 3) or convex upstream (Fig. 5). Their heights range from less than 20 cm to more than 8 m. For reasons discussed below, this class of large-scale bedforms has not been subdivided, and the terms dunes and sand waves are used interchangeably.

'Flat' beds

Beds that appear flat are the second most abundant bottom type observed in the central bay. The theoretical resolution of the side-scan system is approximately 10 cm, and the smallest sand waves visible on the side-scan records are 10–20 cm high. Beds with bedforms less than 10 cm high, small sand waves and all current ripples, would therefore be expected to appear flat.

Although rippled beds are indistinguishable from true flat beds on the side-scan records of the central bay, bed phase can be inferred from depth, velocity, and sediment size. In general, flat-appearing beds in the Golden Gate area are inferred to be upper-flow-regime flat beds because of the high flow velocities; rippled beds probably predominate in other 'flat-bed' areas.

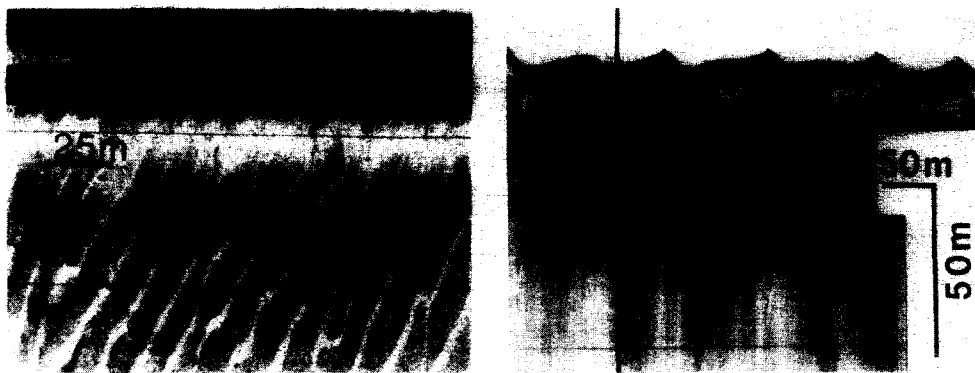


Fig. 3. Side-scan record of straight-crested sand waves. Height is 0.5 m; wavelength is 5–10 m; depth is 20 m; transport from left to right. Location is shown in Fig. 1A.

Fig. 4. Side-scan record of sand waves with reversed crests. Dominant transport is left to right. Sand waves show the effects of right-to-left flow. Maximum height is 5 m; depth is 40 m.

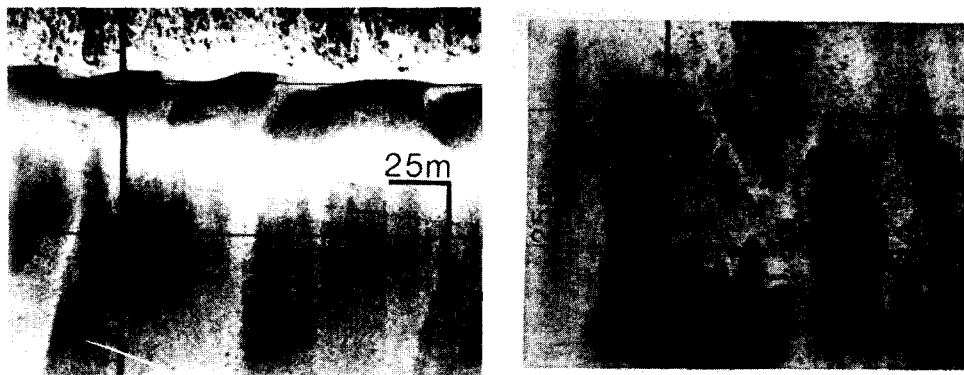


Fig. 5. Side-scan record of three-dimensional sand waves. Maximum height 3 m; water depth 30 m.

Fig. 6. Side-scan record of comet marks. Dark areas are gravel or boulders, light areas are sand; transport from top to bottom.

Bedrock and boulders

Bedrock and boulders occur mostly in the Golden Gate area where fast currents keep the bed swept clear of sand. In some areas, the boulders are numerous enough to form a boulder pavement. In other areas, boulders and bedrock locally protrude through a sand veneer. Turbulence developed at these protuberances downmixes fast moving water and scours the sand veneer to produce rock or boulder-floored sharp pointed depressions (Fig. 6) called comet marks (Werner and Newton, 1975).

DISCUSSION

Bedform equilibrium with tidal flows

In flume experiments designed to produce equilibrium bedforms, flow is regulated until bedforms and flow do not change with time. Hence, observed bedforms are in equilibrium with observed flows. In order to study bedform equilibrium in unsteady natural flows, and to be able to relate observations in natural flows to observations in flumes, sedimentologists have attempted to characterize, by a single velocity, the range of flow velocities in which a specific bed developed in nature. This characterization is a very complicated problem because bedforms respond at different rates, depending both on the rate of sediment transport and the amount of sediment contained in a bedform. In flows where the sediment transport rate is large and bedforms are small, bedforms respond so rapidly that they reflect the flow conditions of as little as a few minutes. In such cases, the bed-molding velocity of the flow

can be approximated by the velocity at which the bedform is observed to be active, a technique employed for bedforms generated by tidal flows (Boothroyd and Hubbard, 1975) and for ripples generated by waves (Dingler and Inman, 1976). Where the volume of sediment contained in a bedform is larger, or where the sediment transport rate is lower, bedforms respond more slowly and may reflect the flow conditions of an entire tide cycle. In these cases, the velocity during peak flow is commonly used to characterize the bed-molding velocity because the sediment transport rate increases as a high power of flow velocity. Consequently, the median and modal sediment transport rates typically occur at velocities greater than 80–90% of the peak flow velocity (Fig. 7).

However, many large sand waves exist at conditions under which weeks, months, or even years of sediment transport are required to modify the bed (Jones et al., 1965; G.P. Allen et al., 1969; J.R.L. Allen and Friend, 1976; Bokuniewicz et al., 1977; Fig. 12, this paper). For these slowly responding bedforms, the peak velocity observed during a randomly selected tide cycle is not an accurate approximation of the bed-molding velocity, because the peak velocity varies from day to day. To accurately characterize the bed-molding velocity in such cases requires calculating the velocity at which the median or modal sediment transport rate occurred during formation of a given bed, and hence, requires knowledge of both the time to form the bed and flow conditions throughout that time.

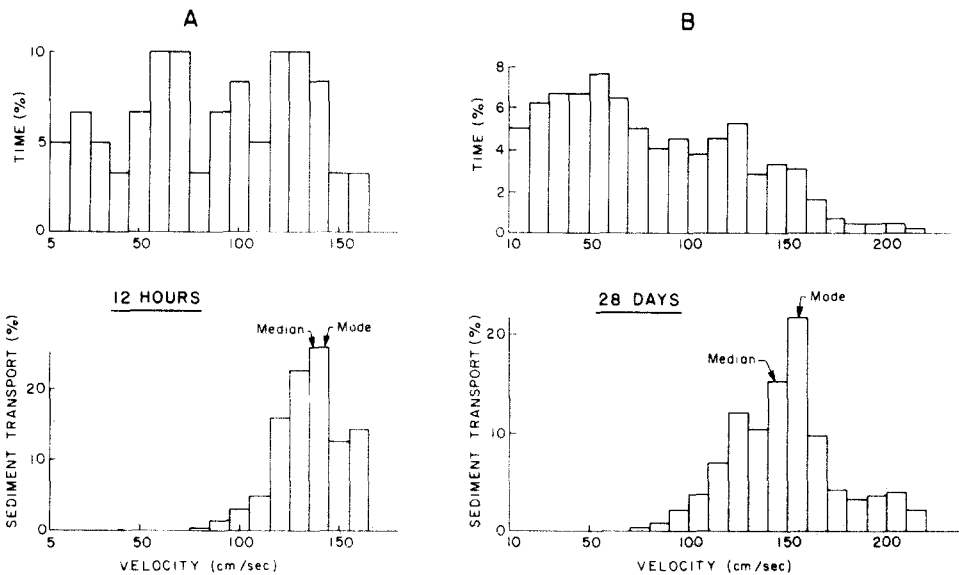


Fig. 7. Histograms of flow duration and sediment transport as a function of flow velocity for a single current meter station. Duration and transport are in percent. Transport was calculated from rates of Colby (1964). A: 12 hours during an average tide; B: 28 days.

For the slowly responding bedforms in the central bay, median and modal transport rates predicted for neap—spring cycles from current-meter records and Colby's (1964) transport rates occur at velocities approximately equal to peak velocities during tides having the mean tide range (Fig. 7). Therefore, peak velocities during average tides (mean tide range $\pm 20\%$) were used to characterize bed-molding velocities in the central bay.

At the locations shown in Fig. 1D, current velocities were measured at two or three depths (near-surface, near-bottom, and mid-water column) by the U.S. Coast and Geodetic Survey for durations of several days to several weeks. Depth-averaged velocities during peak flow of average tides were calculated by plotting velocity profiles on semilog paper and averaging the velocities read from the plot at each tenth of the flow depth.

The velocity characterizations calculated following the procedures given above, or following any other procedure, are subject to errors made in measuring current velocities, errors made in estimating the time required to produce a given bed, and errors made by approximating the range of velocities in which a bed developed by a single velocity. The combined effect of these errors may be 20% or more, and better agreement between the results of this study and previous studies can not be justified and may be somewhat fortuitous.

Bed phase

Velocity—depth (constant grain size) relations. Southard (1971, 1975) identified the flow conditions in which specific bedforms exist, by plotting bed phase as a function of velocity and depth for flume flows up to about 50 cm deep. In Fig. 8, the San Francisco Bay bed-phase observations were combined with those of Southard (1975), Boothroyd and Hubbard (1975), and Dalrymple et al. (1978), and a single set of bed-phase boundaries was drawn from the combined data. The figure shows that within limited grain-size ranges: (1) as depth increases, each bed phase occurs at increasing velocities, and (2) that increasing the velocity produces the same sequence of bed phases as decreasing the depth. It should also be noted that either increasing the velocity or decreasing the depth produces an increase in the shear velocity, a measure of the slope of the velocity profile. For rough turbulent flow where the velocity profile is logarithmic:

$$U_* = \bar{U}/5.75 \log 0.37d/k \quad (1)$$

where U_* is the shear velocity, \bar{U} is the depth-averaged flow velocity, d is the mean flow depth, and k is a measure of the roughness of the bed (Keulegan, 1938, expressed in terms of the depth-averaged velocity). The parallel behavior of bed phase and shear velocity is not coincidental. As shown below, transitions between bed phases, like the initiation of grain movement, appear to occur at critical values of the shear velocity.

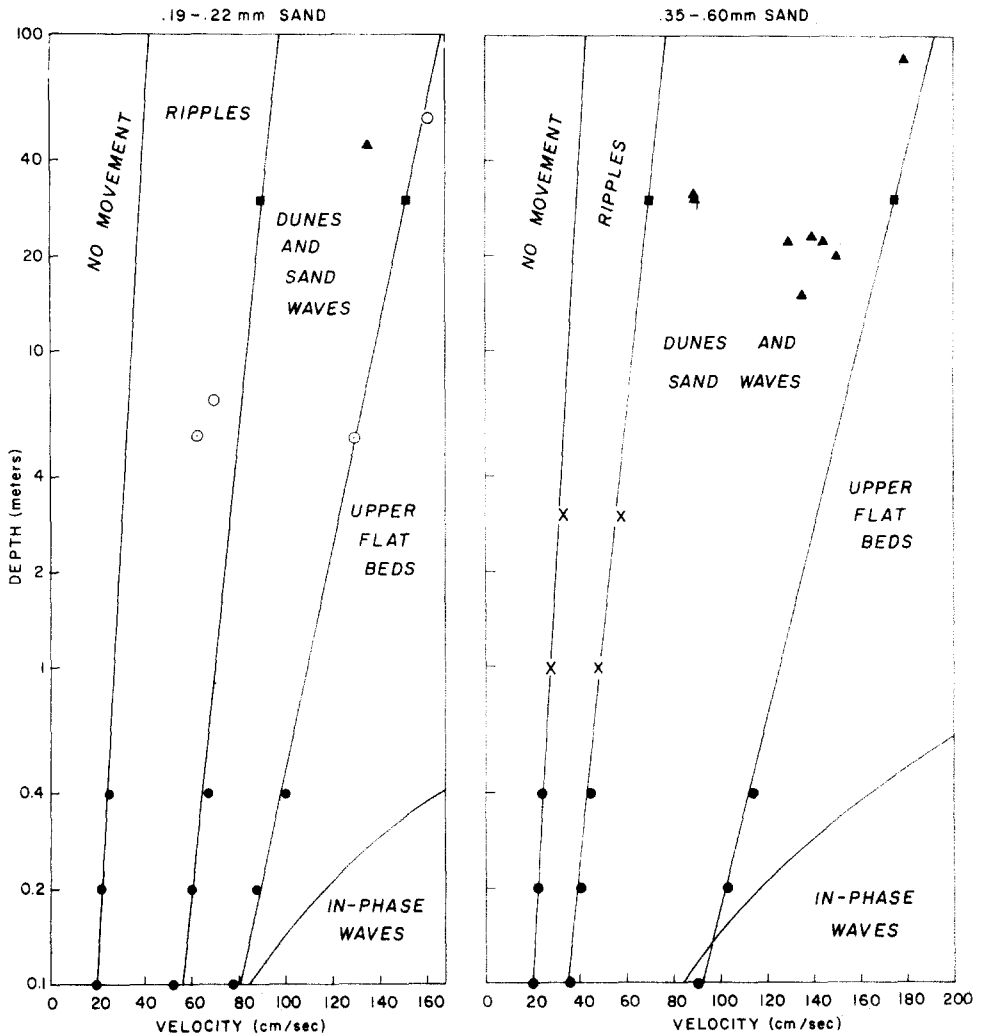


Fig. 8. Semi-log plots of bed phase as a function of depth and velocity for two sediment-size ranges. Triangles and open circles represent San Francisco Bay sand-wave fields and flat-appearing beds, respectively; squares are points on bed-phase boundaries in Fig. 10. Solid circles are points measured or interpolated from bed-phase boundaries determined by Southard (1975, figs. 2-2, 2-3, and 2-5). Crosses and circled dots are points on bed-phase boundaries determined by Boothroyd and Hubbard (1975) and Dalrymple et al. (1978), respectively. Flume velocities are depth-averaged for steady flows; bay velocities are depth-averaged for peak flow during average tides.

Flume studies by Hill et al. (1969), Vanoni (1974), and the flume data collected by Guy et al. (1966) show that the boundaries between the ripple, dune, and upper flat-bed phases occur at critical values of the shear velocity. The values of the critical shear velocities vary with sediment size, but do not

vary detectibly with depth, for the small range of depths attainable in flumes. Calculations based on the San Francisco Bay data suggest that the critical values of the shear velocity remain constant to depths of tens of meters.

The critical values of the shear velocity for the deeper flows were determined using eq. 1 to calculate the maximum shear velocity of flows in equilibrium with ripples and to calculate the minimum shear velocity of flows in equilibrium with upper flat beds. Depth and velocity values used to calculate these critical shear velocities were obtained from coordinates of points on bed-phase boundaries plotted in Fig. 8. The roughness value used in each calculation was the mean roughness, calculated using eq. 1, of all beds with the same sediment size and bed type (ripples or flat bed) in the flume flows of Guy et al. (1966, tables 2 and 5). However, the roughness of each bed type, shown in Table I and Fig. 9, varies so little, that, with the exception of one anomalous flat-bed roughness, choosing *any* of the flume roughness values for the appropriate bed type changes the calculated shear velocity by less than 5%, because of the logarithmic form of eq. 1. Eq. 1 is so insensitive to roughness, that, for a depth of 30 m, changing roughness by a factor of 5 produces a change of less than 20% in calculated shear velocities.

The critical shear velocities calculated using eq. 1, the roughness values used in those calculations, and values for the same critical shear velocities determined by other studies are shown in Table I. The good agreement between the values observed in shallow flows and the values calculated for the deeper flows suggests that the critical shear velocities listed in Table I are constant for flows ranging in depth from tens of centimeters to tens of meters.

As Southard (1975) noted, the transition from sand waves to upper flat beds is accompanied by a decrease in shear velocity caused by a decrease in

TABLE I

Comparison of calculated and observed critical shear velocities for bed-phase changes

Sediment size (mm)	Bed-phase change	k used to calculate U_* (cm)	Critical shear velocities, U_{*cr} (cm/sec)			
			1 calculated	2 observed	3 observed	4 observed
0.2	ripples—dunes	0.1	3.9	3.6	4.2	4.4
0.2	flat beds—dunes	0.002	4.6	3.9	5.1	—
0.5	ripples—dunes	0.1	3.1	3.2	3.5	3.4
0.5	flat beds—dunes	0.008	5.9	6.9	6.1	—

¹ U_{*cr} is maximum predicted equilibrium ripple shear velocity or minimum upper flat-bed shear velocity; ² Hill et al. (1969); U_{*cr} is minimum upper flat-bed shear velocity; ³ Guy et al. (1966); maximum observed ripple shear velocity; ⁴ Vanoni (1974, fig. 7); U_{*cr} is mean shear velocity at ripple-dune phase change.

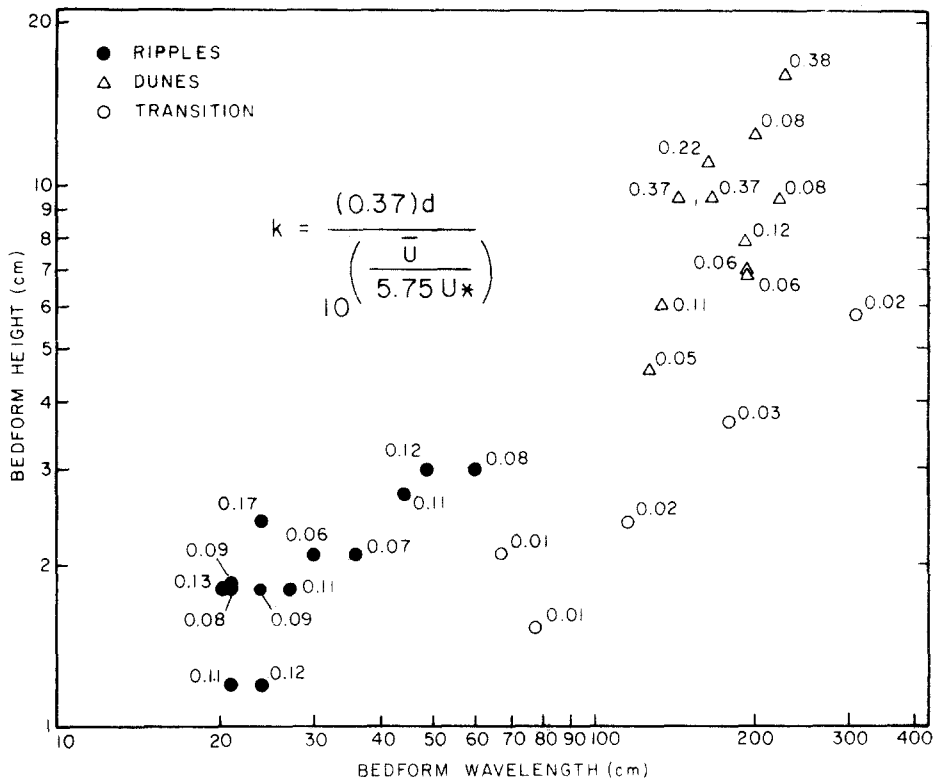


Fig. 9. Log-log plot of bed roughness, k , as a function of bedform height and wavelength for all ripple, dune, and transition flows over 0.45-mm sand beds in Guy et al. (1966, table 5). For a given bedform height, roughness decreases as wavelength increases.

bed roughness. At depths of several tens of centimeters, maximum sand-wave shear velocities are approximately 7 cm/sec for 0.19 mm sand and 9 cm/sec for 0.45 mm sand (Guy et al., 1966, tables 2 and 5). Maximum sand-wave shear velocities in deeper flows can be calculated using eq. 1, which states that the shear velocity of a flow is proportional to the mean velocity and inversely proportional to the log of the relative roughness, $0.37 d/k$, of the flow. Increasing the flow depth from 20 cm to 30 m increases by a factor of 2 the velocities at which sand waves are stable (Fig. 8), but the log of the relative roughness can be expected to remain relatively constant. As a result, the upper limit of *equilibrium* sand-wave shear velocities in 30 m deep flows can be expected to be approximately twice that of 20 cm deep flows. Thus, maximum ripple shear velocities and minimum upper flat-bed shear velocities do not appear to vary with depth, but maximum sand-wave shear velocities do vary because *maximum* sand-wave size increases with flow depth.

Because the slope of a logarithmic velocity profile is equal to $(5.75 U_*)^{-1}$ and the y-intercept equal to the log of the bed roughness, all logarithmic



Erratum

Rubin, D.M. and McCulloch, D.S., 1980. Single and superimposed bedforms: a synthesis of San Francisco Bay and flume observations. *Sediment. Geol.*, 26: 207–231.

The authors submitted the wrong Fig. 10. The following correct figure is based on the methods discussed in the text and on the data given in Figs. 1A–1D and listed in the Appendix.

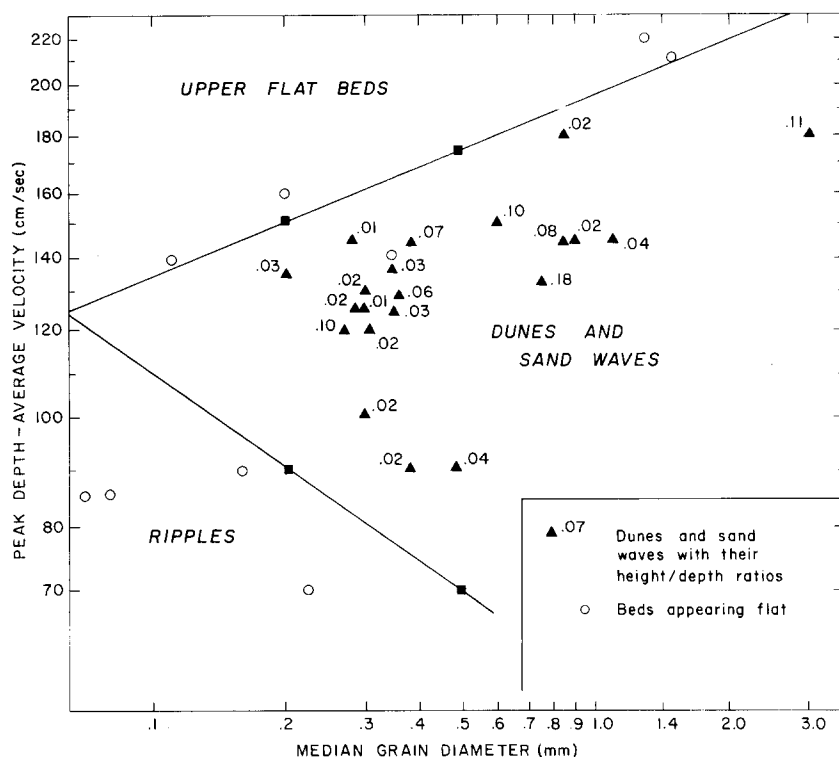


Fig. 10. Log-log plot of bed phase as a function of sediment size and velocity for flow depths on the order of 30 m. Each point represents an entire bedform field listed in the Appendix. Squares are points on bedphase boundaries in Fig. 8.

system used to survey the bay was unable to detect ripples or other bedforms less than about 10 cm high. In deep water, each bed phase occurs at higher velocity than in shallow flows, because in the deeper flows, a higher depth-averaged velocity is required to produce the same shear velocity over any given bed.

Sand-wave height

Depth. Equilibrium sand-wave height, like bed phase, is determined largely by depth, velocity, and sediment size. Of these parameters, depth is the best documented control of sand-wave height. Field, analytical, and flume studies have shown that at depths greater than several tens of centimeters the mean height of relatively straight-crested sand waves in a train is generally *less than or equal to* approximately 1/6 of the mean flow depth (Allen, 1963; Yalin, 1964; Stein, 1965). Similarly, in San Francisco Bay the greatest height/depth ratio is 1/6. Although the flow depth is an important limit of sand-wave height, it is not the sole control. As will be discussed below, velocity and sediment size also control sand-wave height, and sand waves need not be as high as 1/6 of the flow depth if the velocity and sediment size are not optimum. More typically, velocity and grain size are less than optimum in San Francisco Bay, and height/depth ratios are generally 1/10 to 1/50. Similarly, Bokuniewicz et al. (1977) observed height/depth ratios ranging from approximately 1/5 to less than 1/100.

Velocity. Yalin (1964) predicted mathematically and demonstrated experimentally that the height/depth ratio, H/d , of sand waves is proportional to the dimensionless excess tractive force:

$$H/d = 1/6[(\tau_0 - \tau_{cr})/\tau_0] \quad (2)$$

where τ_0 is the shear stress on the bed and τ_{cr} is the critical shear stress for the initiation of grain movement (Yalin, 1964, eqs. 7 and 13 combined). Increasing the flow velocity over a sand wave field will increase the shear stress on the bed, τ_0 , and produce larger sand waves. Qualitatively, the same relationship has been observed by Stein (1965), Znamenskaya (1966), J.R.L. Allen (1968, fig. 4.7), G.P. Allen et al. (1969), Coleman (1969), Pratt and Smith (1972), Jackson (1975), and is suggested by McCave's (1971) modified version of Kennedy's (1969) equation of sand-wave height:

$$H = \frac{LB}{n} \frac{(\bar{U} - \bar{U}_c)}{\bar{U}} \tanh \frac{2d}{L} \quad (3)$$

where L is sand-wave wavelength, n is a constant, \bar{U}_c is the critical mean velocity for the initiation of grain movement, and B is the ratio of the rate of transport of sediment composing the bedform to the total sediment transport rate. Eq. 3 is compatible with the interpretation that an increase in velocity produces an increase in sand-wave height, until the suspended-sedi-

ment transport rate becomes large with respect to the bedload transport rate (B decreases) causing sand-wave height to decrease. As velocity continues to increase, sand-wave height eventually decreases to zero, and the sand-wave phase is replaced by the upper flat-bed phase.

The height of sand waves in San Francisco Bay also appears to be a function of velocity. Although the current-velocity stations are too widely spaced to measure velocity changes across single sand-wave trains, sand waves with large height/depth ratios generally occur at higher velocities within the sand-wave phase (Fig. 10).

Sediment size. In San Francisco Bay, the largest height/depth ratios are restricted to relatively coarse-grained sand waves. Bay sand waves with height/depth ratios greater than 1/10 are common in sediments with median grain diameters greater than 0.5 mm but rare in finer sediment.

McCave (1971), studying bedforms in the North Sea, also observed that sand-wave height decreased with sediment size. He attributed the decrease in height to an increase in the rate of suspended-sediment transport (a decrease in B in eq. 3). Similarly, Dalrymple et al. (1978) observed that in the Bay of Fundy the largest bedforms occur in sand coarser than 0.3 mm. However, in the flume data collected by Guy et al. (1966), and in a plot of flume data by Znamenskaya (1966), maximum sand-wave height does not appear to increase with sediment size. This difference between the field and flume observations may be the result of the greater unsteadiness of tidal flows. The velocity fluctuations which occur in a tidal flow could be expected to be more destructive to a fine-grained sand wave than to a coarse-grained sand wave, because as grain size decreases, the range of velocities at which sand waves are stable narrows (Fig. 10). Thus, the relation between sand-wave height and sediment size observed in natural flows may be a result of large-scale velocity fluctuations not present in flume flows.

A three-dimensional plot of bed phase and sand-wave height is shown in Fig. 11. The plot is generalized from the bay and flume data cited above, and all trends illustrated have been observed by more than one experimenter. As in all bed-phase plots, the data are subject to scatter caused by variations in parameters that were not considered in the plot. For example, two flows with identical depths and depth-averaged velocities can exert different shear stresses on the bed, because the flows can have different water temperatures, deviations from logarithmic velocity profiles, or different concentrations of suspended sediment. Similarly, two sediments with the same median grain diameter but different sorting, skewness, density, or shape may form different bed configurations in flows with the same mean depth and velocity.

Equilibrium superimposed bedforms

Superimposed bedforms are common in both flume and natural flows. In some cases, superimposed bedforms develop in response to temporal flow

In each of the 18 cases where they observed ripples or sand waves, the bed-forms were contained in a flow layer having a thickness of several bedform heights. In 16 of the 18 cases, the shear velocities of the flow layers were within 10% of the ranges predicted from Table I for the observed bedforms and sediment size.

Shear velocity can vary with height above the bed because what might be thought of as an effective hydraulic roughness varies with height above the bed. Away from the bed, the roughness is that associated with large bed-forms. Approaching the bed, the surface of a large bedform approximates a flat bed, and the roughness decreases to that associated with smaller superimposed bedforms or individual grains. This decrease in roughness in the vicinity of the bed decreases the intercept of the velocity profile, which in turn increases the slope of the velocity profile, and produces a decrease in the shear velocity near the bed. At these lower shear-velocity conditions near the bed, ripples, sand waves, or flat beds can exist on larger bedforms. In effect, large bedforms generate boundary layers in which smaller bedforms can exist.

The shear velocity in the flow near a bed varies across the surface of a large bedform from a minimum near the trough to a maximum near the crest. This variation has been measured in flumes (Raudkivi, 1966) and in natural flows (McLean, 1976). The effect of this variation on the distribution of superimposed bedforms has been observed by Guy et al. (1966), McCave (1971), and Harms et al. (1974). Guy et al. (1966) observed that in flows with shear velocities low in the sand-wave range, ripples covered sand-wave stoss slopes. At shear velocities that are higher in the sand-wave range, upper flat-beds formed at sand-wave crests and ripples were restricted to lower shear-velocity flow in the troughs. Similarly, Harms et al. (1974) observed a trough-to-crest sequence of algae-stabilized flat beds to ripples to small sand waves, superimposed on larger sand waves, and McCave (1971, fig. 5D) observed a trough-to-crest increase in size of superimposed bedforms. Thus, the supposition that bed phase is a function of shear velocity is quantitatively supported by Smith and McLean's (1977) observations of vertical variations in shear velocity over superimposed bedforms and qualitatively supported by observed trough-to-crest variations in shear velocity and superimposed bedforms.

Sediment transport rates

Because both the rate of sediment transport and bed phase are functions of velocity, depth, and sediment size, they can be directly compared. In Fig. 12, empirically determined and extrapolated sediment transport rates from Colby (1964) are superimposed on bed-phase plots. These plots give an estimate of the rate of sediment transport for flows in equilibrium with specified beds. According to Colby (1964), approximately three fourths of predicted transport rates are within a factor of 2 of observed rates. Poorest

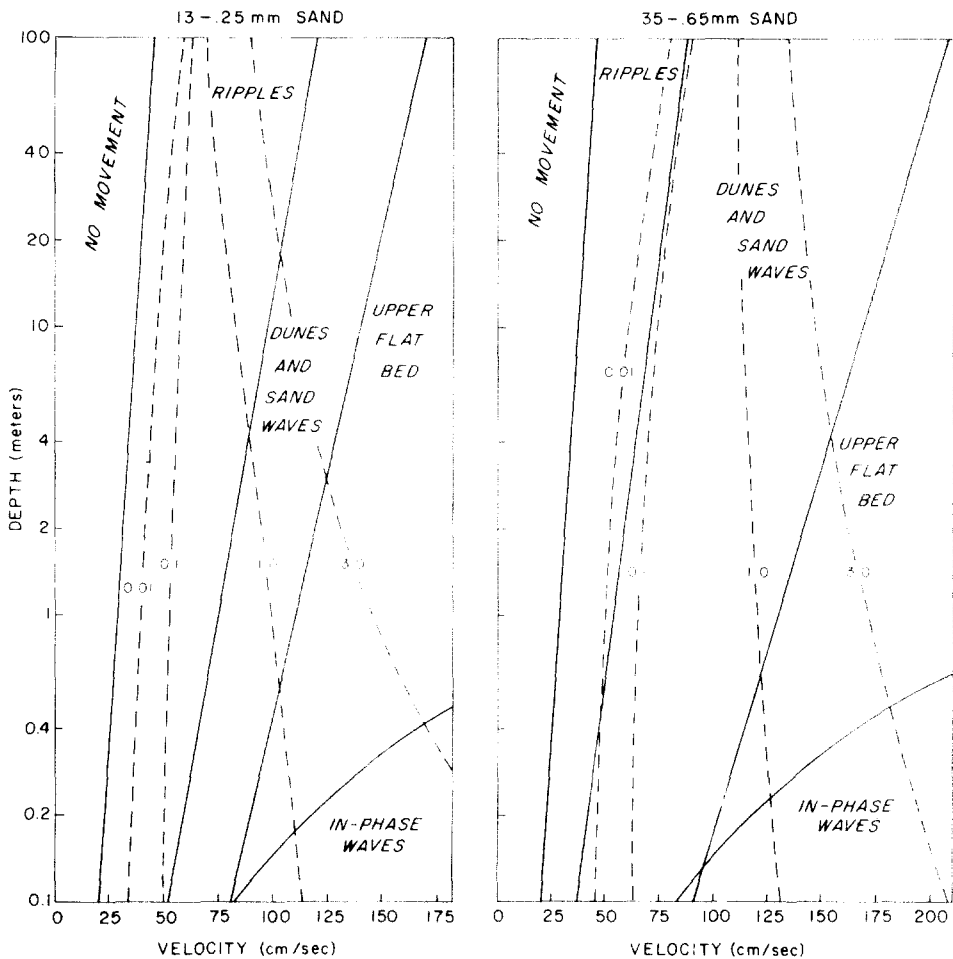


Fig. 12. Semi-log plot of bed phase and sediment transport rate (dashed lines) as functions of depth and velocity. Transport rates, in $\text{kg/m} \cdot \text{sec}$, are from Colby (1964).

agreement is for shallow depths, low velocities, and rates measured in flumes. Predicted transport rates for flows deeper than approximately 3 m are largely extrapolated, and Colby did not specify the accuracy of those rates.

For any constant depth and sediment size, the sediment transport rate increases with flow velocity. As discussed above, dune height also increases with flow velocity. Consequently, at any one depth, big dunes are generated by flows having high sediment transport rates. As a result, where dunes are in equilibrium with flows having the same depth, big dunes migrate faster than small dunes. This trend is the opposite of what would be predicted if the dependence of dune height on flow velocity was overlooked. The increase in migration rate as a function of increasing dune height is very

clearly illustrated in the flume data of Guy, Simons, and Richardson (1966). In flows that are transitional with upper flat beds, however, this trend reverses, because dune height decreases as flow velocity and the rate of sediment transport increase.

Where depth is not constant, the relation of dune height to migration speed is more complex. The maximum height of dunes in 100-m-deep flows is approximately three orders of magnitude larger than the maximum height in 0.1-m-deep flows, but the sediment transport rate in the deeper flows is only one or two orders of magnitude larger than in shallow flows. Thus, where equilibrium dune height increases because of a depth increase, dune migration speed decreases.

Bedform terminology

Some sedimentologists have subdivided the group of large-scale bedforms that form in 0.3–0.5 mm sand into various classes of megaripples, dunes, and sand waves on the basis of size (Coleman, 1969; Boothroyd and Hubbard, 1975), morphology (Znamenskaya, 1963; Allen, 1968; Hine, 1975; Southard, 1975), or both (Dalrymple et al., 1978). These authors have demonstrated that as the flow over a bed increases in velocity or decreases in depth, the crests of large-scale bedforms become sinuous in plan view, and scour pits develop in bedform troughs (in Allen's terminology the bedforms become three-dimensional).

The relatively straight-crested, two-dimensional bedforms that, for a given depth, form at flow velocities higher than ripples, but less than taller three-dimensional bedforms, have been called flat dunes (Znamenskaya, 1963), flattened dunes (Pratt and Smith, 1972), linear megaripples (Boothroyd and Hubbard, 1975; Hine, 1975), bars (Costello, 1974), type-I megaripples (Dalrymple et al., 1978), and two-dimensional dunes (Southard and Costello, in preparation). The terminology is complicated not merely because different names are used for what appear to be the same kind of bedform, but because size has been used to distinguish bedform classes, and the maximum height and wavelength of both two- and three-dimensional bedforms increase with the scale of the flow. For example, bedforms belonging to the class called flat dunes, etc., increase in height from 1 to 2 cm in flows 8 cm deep (Pratt and Smith, 1972), to heights of 5–20 cm in flows approximately 1 m deep (Hine, 1975), to heights of 5–50 cm in flows on the order of 6 m deep (Dalrymple et al., 1978) to heights of 2 m in San Francisco Bay flows 20 m deep. Maximum wavelength also increases with flow depth.

Similarly, the maximum height of three-dimensional bedforms increases from 20 cm high dunes in flume flows up to 50 cm deep (Southard, 1975), to 70 cm high type-II megaripples in Bay of Fundy flows on the order of 6 m deep (Dalrymple et al., 1978), to 2–3 m high bedforms in flows 10–30 m deep in San Francisco Bay (Fig. 5), in the Brahmaputra River (Coleman, 1969, fig. 25B), and in Willapa Bay (Phillips, 1979). These observations sug-

gest that large bedforms produced by deep natural flows are the same kinds of bedforms as those produced in shallow flume and natural flows. Until future observations demonstrate that large dunes and small dunes with similar crest shapes and sediment sizes are different populations of bedforms and are generated by different mechanisms, then the classification of dunes by size is likely to result in artificial separation of genetically related beforms.

Height/wavelength ratios have been used to demonstrate that bedforms distinguished by less easily quantifiable characteristics, such as degree of three-dimensionality, are actually different kinds of bedforms. In many cases, however, height/wavelength ratios are not useful in identifying individual bedforms because two or more kinds of bedforms can have the same ratio. The more promising approach seems to be to classify bedforms by morphological characteristics such as degree of three-dimensionality.

CONCLUSIONS

(1) Bed configuration in San Francisco Bay, as in flumes, is a function of sediment size, velocity, and flow depth.

(2) Comparison of bedform sequences suggests that, for flows up to tens of meters deeps, beds of 0.25–0.50 mm sand respond to increasing flow velocities by forming ripples, two-dimensional sand waves, three-dimensional sand waves, and flat beds. At any constant depth, the two-dimensional bedforms stable at low velocities tend to be smaller than the three-dimensional

APPENDIX

Observations

Location (from Fig. 1C)	Median grain diameter (mm)	Depth (m)	Peak depth-averaged velocity (cm/sec)	Bedform height (m)
1	1.1	35	145	1.3
2	0.9	52	145	0.1
3	3.1	55	180	6
4	0.6	85	180	2
5	0.2	55	160	none
6	1.3	70	220	none
7	1.5	45	210	none
8	0.27	20	120	2
9	0.85	20	145	1.5
10	0.60	20	150	2
11	0.38	22	145	1.5
12	0.30	27	130	0.5
13	0.35	15	135	0.5
14	0.36	23	140	none

APPENDIX (continued)

Location (from Fig. 1C)	Median grain diameter (mm)	Depth (m)	Peak depth-averaged velocity (cm/sec)	Bedform height (m)
15	0.28	34	145	0.3
16	0.11	11	140	none
17	0.29	24	125	0.5
18	0.31	26	120	0.5
19	0.30	37	125	0.4
20	0.20	45	135	1.2
21	0.36	22	130	1.2
22	0.34	16	125	0.5
23	0.29	19	100	0.4
24	0.37	30	90	0.6
25	0.47	31	90	1.2
26	0.16	8	90	none
27	0.08	7	85	none
28	0.07	7	85	none
29	0.22	7	70	none
30	0.75	22	130	4

bedforms stable at higher velocities, but the maximum height of both kinds of bedforms increases with the scale of the flow.

(3) For depths from tens of centimeters to tens of meters, maximum shear velocities of flows in equilibrium with ripples and minimum shear velocities of flows in equilibrium with upper flat beds appear to be constant for a given sediment size. Maximum sand-wave shear velocities increase with flow depth.

(4) Large bedforms generate boundary layers in which ripples, dunes, and/or flat beds exist.

(5) Velocity measurements used to characterize the flow that generated an observed bed must be made on spatial and temporal scales of the flow that generated the bedform.

ACKNOWLEDGEMENTS

Ralph Hunter discussed ideas, suggested references, and read the manuscript. Arnold Bouma, David Caccione, and John Southard read the manuscript and offered helpful comments. Paul Carlson supplied unpublished grain-size data. Part of this work was supported by a National Research Council Postdoctoral Research Associateship for David Rubin.

REFERENCES

- Allen, G.P., Deresseguier, A. and Klingebiel, A., 1969, Evolution des structures sedimentaires sur un banc sableux d'estuaire en fonction de l'amplitude des mares. C.R. Acad. Sci., D269: 2167-2169.

- Allen, J.R.L., 1963. Asymmetrical ripple marks and the origin of water-laid cosets of cross-strata. *Liverpool Manchester Geol. J.*, 3: 187–236.
- Allen, J.R.L., 1968. *Current Ripples: Their Relation to Patterns of Water and Sediment Motion*. North-Holland, Amsterdam, 433 pp.
- Allen, J.R.L., 1978. Polymodal dune assemblages: an interpretation in terms of dune creation—destruction in periodic flows. *Sediment. Geol.*, 20: 17–28.
- Allen, J.R.L. and Friend, P.F., 1976. Relaxation time of dunes in decelerating aqueous flows. *J. Geol. Soc. London*, 132: 17–26.
- Bokuniewicz, H.J., Gordon, R.B. and Kastens, K.A., 1977. Form and migration of sand waves in a large estuary, Long Island Sound. *Mar. Geol.*, 24: 185–199.
- Boothroyd, J.C. and Hubbard, D.K., 1975. Genesis of bedforms in mesotidal estuaries. In: L.E. Cronin (Editor), *Estuarine Research*. Acad. Press, New York, N.Y., pp. 217–234.
- Colby, B.R., 1964. Discharge of sands and mean-velocity relationships in sand-bed streams. *U.S. Geol. Surv. Prof. Pap.*, 462-A: 47 pp.
- Coleman, J.M., 1969. Brahmaputra River: channel processes and sedimentation. *Sediment. Geol.*, 3: 129–239.
- Costello, W.R., 1974. Development of bed configurations in coarse sands. *Mass. Inst. Technol. Dep. Earth Planet. Sci. Rep.*, 74-1: 120 pp.
- Dalrymple, R.W., Knight, R.J. and Lambiase, J.J., 1978. Bedforms and their hydraulic stability relationships in a tidal environment, Bay of Fundy, Canada. *Nature*, 275: 100–104.
- Dingler, J.R. and Inman, D.L., 1976. Wave-formed ripples in nearshore sands. *Proc. 15th Coast. Eng. Conf. ASCE*, Honolulu, Hawaii, pp. 2109–2126.
- Guy, H.P., Simons, D.B. and Richardson, E.V., 1966. Summary of alluvial channel data from flume experiments, 1956–1961. *U.S. Geol. Surv. Prof. Pap.*, 462-I: 96 pp.
- Harms, J.C., 1969. Hydraulic significance of some sand ripples. *Geol. Soc. Am. Bull.*, 80: 363–396.
- Harms, J.C., Choquette, P.W. and Brady, M.J., 1974. Carbonate sand waves, Isla Mujeres, Yucatan. In: A.E. Weidie (Editor), *Field Seminar on Water and Carbonate Rocks of the Yucatan Peninsula, Mexico*. *Geol. Soc. Am. Annu. Meet.*, Miami, Fla., pp. 123–147.
- Hill, H.M., 1966. Bed forms due to a fluid stream. *Proc. Am. Soc. Civ. Eng., J. Hydraul. Div.*, 92: 127–143.
- Hill, H.M., Srinivasan, V.S. and Unny, T.E., Jr., 1969. Instability of flat bed in alluvial channels. *Proc. Am. Soc. Civ. Eng., J. Hydraul. Div.*, 95: 1545–1558.
- Hine, A.C., 1975. Bedform distribution and migration patterns on tidal deltas in the Chat-ham Harbor estuary, Cape Cod, Massachusetts. In: L.E. Cronin (Editor), *Estuarine Research*, Acad. Press, New York, N.Y., pp. 235–252.
- Jackson, R.G., 1975. Hierarchical attributes and a unifying model of bedforms composed of cohesionless material and produced by shearing flow. *Geol. Soc. Am. Bull.*, 86: 1523–1533.
- Jones, N.S., Kain, J.M. and Stride, A.H., 1965. The movement of sand waves on Warts Bank, Isle of Man. *Mar. Geol.*, 3: 329–336.
- Keulegan, G.H., 1938. Laws of turbulent flow in open channels. *U.S. Natl. Bur. Stand. Res. J.*, 21: 707–741.
- Kennedy, J.F., 1969. The formation of sediment ripples, dunes, and antidunes. *Annu. Rev. Fluid Mech.*, 1: 147–168.
- McCave, I.N., 1971. Sand waves in the North Sea off the coast of Holland. *Mar. Geol.*, 10: 199–225.
- McLean, S.R., 1976. *Mechanics of the Turbulent Boundary Layer over Sand Waves in the Columbia River*. Ph.D. thesis, Univ. of Washington, Seattle, 231 pp.
- Phillips, R.L., 1979. Bed forms and processes on estuarine tidal-current ridge, Willapa Bay, Washington. *Program Am. Assoc. Pet. Geol. Annu. Meet.*, Houston, Texas, p.145.

- Pratt, C.J. and Smith, K.V.H., 1972, Ripple and dune phases in a narrowly graded sand. *Proc. Am. Soc. Civ. Eng., J. Hydraul. Div.*, 98: 859—874.
- Raudkivi, A.J. 1966. Bed forms in alluvial channels. *J. Fluid Mech.*, 26: 507—514.
- Rubin, D.M. and McCulloch, D.S., 1976. Bedform dynamics in San Francisco Bay, California. *Geol. Soc. Am. Abstr. Program*, 8: 1079.
- Simons, D.B., Richardson, E.V. and Nordin, C.F., Jr., 1965. Sedimentary structures generated by flow in alluvial channels. In: G.V. Middleton (Editor), *Primary Sedimentary Structures and their Hydrodynamic Interpretation*. Soc. Econ. Paleontol. Mineral. Spec. Publ., 12: 34—52.
- Smith, J.D. and McLean, S.R., 1977. Spatially averaged flow over a wavy surface. *J. Geophys. Res.*, 82: 1735—1746.
- Southard, J.B., 1971. Representation of bed configurations in depth-velocity-size diagrams. *J. Sediment. Petrol.*, 41: 903—915.
- Southard, J.B., 1975. Bed configurations. In: *Depositional Environments as Interpreted from Primary Sedimentary Structure and Stratification Sequences*. Soc. Econ. Paleontol. Mineral., Short Course, 2: 5—43.
- Stein, R.A., 1965. Laboratory studies of total load and apparent bed load. *J. Geophys. Res.*, 70: 1831—1842.
- U.S. Coast and Geodetic Survey. Unpublished current-meter data for San Francisco Bay, available from National Ocean Survey, Rockville, Md.
- Vanoni, V.A., 1974. Factors determining bed forms of alluvial streams. *Proc. Am. Soc. Civ. Eng., J. Hydraul. Div.*, 100: 363—377.
- Werner, F. and Newton, R.S., 1975. The pattern of large-scale bed forms in the Langeland Belt (Baltic Sea). *Mar. Geol.*, 19: 29—59.
- Yalin, M.S., 1964. Geometrical properties of sand waves. *Proc. Am. Soc. Civ. Eng., J. Hydraul. Div.*, 90: 105—119.
- Znamenskaya, N.S., 1963. Experimental study of the dune movement of sediment. *Sov. Hydrol., Select. Pap.*, 3: 253—275.
- Znamenskaya, N.S., 1966. Experimentation on erodible models. *Sov. Hydrol., Select. Pap.*, 6: 477—486.